Research Article
Open Access
Life Sciences, Medicine and Biomedicine

Development and characterization of mesalamine-loaded nano-ZIF-8 via controlled-stirring synthesis

Nur Airin Syahira Johari[1], Gaayatri Silvaraju[1], Mohd Akmal Azhar[1], Azren Aida Asmawi[2], Rosniza Razali[3] and Nurul Akmarina Mohd Abdul Kamal[1,*]

[1]*PharmTech Cluster, Faculty of Chemical and Process Engineering Technology, Universiti Malaysia Pahang Al-Sultan Abdullah (UMPSA), 26300 Gambang, Pahang, Malaysia.*
[2]*School of Pharmacy, Faculty of Pharmacy and Biomedical Sciences, MAHSA University, Bandar Saujana Putra, 42610 Jenjarom, Selangor, Malaysia.*
[3]*Medical Technology Division, Malaysian Nuclear Agency, 43000 Kajang, Selangor, Malaysia.*

**Correspondence: nurulakmarina@umpsa.edu.my*

Received 24 September 2025; Revised 16 December 2025; Accepted 20 January 2026; Published online 8 March 2026

ABSTRACT

Mesalamine (MES), widely prescribed for inflammatory bowel disease (IBD) and explored for cancer repurposing, exhibits limited stability and non-selective biodistribution, emphasizing the need for efficient carrier systems to enhance the efficacy of the carrier system, it is necessary to control the drug loading during the synthesis procedure. Therefore, in this study, we synthesized mesalamine-loaded ZIF-8 nanoparticles (MES@nZIF-8) via a controlled-stirring approach and to assess the effect of reaction time (15 min, 24 h, 48 h, 72 h) on the MES loading and its physicochemical properties. Successful characterization techniques were proven by spectroscopic and electron microscopic procedure. A change from milky white to pale yellow was observed with longer stirring. Powder X-ray diffraction (PXRD) patterns matched simulated ZIF-8, indicating retained framework crystallinity across conditions. Fourier transformed infrared (FTIR) spectroscopy showed distinct band shifts at 1674 cm^{-1}, 2359 cm^{-1}, and 2341 cm^{-1} at 48 h, consistent with enhanced drug–framework interactions at 48 h. Scanning electron microscope (SEM) and dynamic light scattering (DLS) revealed that particle size increased from 91.2 ± 10.77 nm (pristine nZIF-8) to 169.37 ± 25.86 nm (MES@nZIF-8) at 48 h, with hydrodynamic size rising from 229.97 ± 0.74 nm to 266.70 ± 4.32 nm, respectively. Meanwhile, thermal stability (TGA) declined with increasing reaction time. The highest EE (95.35 ± 0.02%) and DL (10.17%) were achieved at 48 h. These findings suggests that reaction time significantly modulates the physicochemical characteristics and stability of MES@nZIF-8, offering insight into the design of anti-inflammatory drug-loaded MOFs for pH-responsive drug delivery applications.

Keywords: *Cancer; drug delivery; mesalamine; ZIF-8 and reaction*

INTRODUCTION

Cancer continues to present significant therapeutic challenges, in part due to the limitations of conventional chemotherapeutics whose nonspecific distribution contributes to considerable toxicity in healthy tissues (Chehelgerdi et al., 2023; Zafar et al., 2025). Among emerging strategies to address backs, the repurposing of anti-inflammatory agents with chemopreventive properties has attracted increasing attention (Khalil et al., 2024; Kolawole & Kashfi, 2022; Lai et al., 2022; Ozleyen et al., 2023; Tunc et al., 2023). Mesalamine (MES) or 5-aminosalicylic acid (5-ASA), has been widely used in the management of inflammatory bowel disease (IBD), exerting its therapeutic effect primarily through inhibition of cyclooxygenase pathways and suppression of pro-inflammatory cytokines (Beiranvand, 2021). Preclinical studies have established that mesalamine exerts antiproliferative and pro-apoptotic effects on colorectal carcinoma and breast cancer cell lines, inducing cell cycle arrest and caspase-dependent apoptosis at micromolar concentrations (Słoka et al., 2023). Notably, longitudinal data suggest that chronic mesalamine use is associated with reduced

https://doi.org/10.28916/lsmb.10.1.2026.227

neoplastic transformation in ulcerative colitis (UC) patients, reinforcing its promise as an adjunct anticancer agent (Słoka et al., 2023). Its excellent safety profile, characterized by rare severe adverse events and generally mild side effects, further underscores its suitability for sustained oncologic application (Liefferinckx et al., 2019).

Cancer continues to present significant therapeutic challenges, in part due to the limitations of conventional chemotherapeutics whose nonspecific distribution contributes to considerable toxicity in healthy tissues (Chehelgerdi et al., 2023; Zafar et al., 2025). Among emerging strategies to address backs, the repurposing of anti-inflammatory agents with chemopreventive properties has attracted increasing attention (Khalil et al., 2024; Kolawole & Kashfi, 2022; Lai et al., 2022; Ozleyen et al., 2023; Tunc et al., 2023). Mesalamine (MES) or 5-aminosalicylic acid (5-ASA), has been widely used in the management of inflammatory bowel disease (IBD), exerting its therapeutic effect primarily through inhibition of cyclooxygenase pathways and suppression of pro-inflammatory cytokines (Beiranvand, 2021). Preclinical studies have established that mesalamine exerts antiproliferative and pro-apoptotic effects on colorectal carcinoma and breast cancer cell lines, inducing cell cycle arrest and caspase-dependent apoptosis at micromolar concentrations (Słoka et al., 2023). Notably, longitudinal data suggest that chronic mesalamine use is associated with reduced neoplastic transformation in ulcerative colitis (UC) patients, reinforcing its promise as an adjunct anticancer agent (Słoka et al., 2023). Its excellent safety profile, characterized by rare severe adverse events and generally mild side effects, further underscores its suitability for sustained oncologic application (Liefferinckx et al., 2019).

In parallel with investigations into therapeutic repurposing, nanocarrier-based delivery technologies have evolved to improve drug accumulation within tumor microenvironments and limit systemic exposure (Cheng & Xu, 2020; Haripriyaa & Suthindhiran, 2023; Lim et al., 2019; Ortega et al., 2020; Yao et al., 2020). Among these, zeolitic imidazolate framework-8 (ZIF-8) has gained prominence as a pH-responsive platform capable of encapsulating diverse small molecules and releasing them selectively under acidic conditions (Kumari et al., 2023; Obaid et al., 2022; Xie et al., 2022). This pH-responsive behavior is particularly due to the tumor microenvironment is characteristically acidic (pH ~6.5–6.9) compared to normal tissues (pH ≈ 7.4), as a consequence of high glucose consumption, lactate production, and hypoxia in cancer cells (Estrella et al., 2013; Tafech & Stéphanou, 2024; Webb et al., 2011). Such acidic environment enables ZIF-8 to undergo structural degradation and release the drug specifically at the tumor site. In addition, the crystalline architecture and tunable porosity of ZIF-8 enable high drug loading, while its intrinsic biocompatibility supports its application in cancer nanomedicine. Furthermore, metal–organic frameworks (MOFs) like ZIF-8 exhibit superior capacity to encapsulate polar compounds within their lattice, with studies reporting encapsulation yields exceeding 80% under optimized conditions (Amur et al., 2023). Additionally, nanoparticles capitalize on the enhanced permeability and retention (EPR) effect, favoring passive accumulation within tumor vasculature while reducing clearance by the mononuclear phagocyte system (Kalyane et al., 2019; Vagena et al., 2025). In contrast, although polymeric micelles and liposomes can solubilize hydrophilic drugs such as mesalamine, their encapsulation efficiency and retention are often limited by premature leakage and instability (Biswas, 2021; Qian et al., 2023). This limitation is often attributed to weak drug–carrier interactions, where hydrophilic molecules show poor affinity for the hydrophobic micelle core or lipid bilayer, leading to loss of stability and early drug release in physiological media (Chelliah et al., 2025).

Despite these advances, there remains a critical need to establish synthesis protocols that reliably control ZIF-8 particle characteristics and maximize therapeutic loading. Stirring conditions during synthesis have emerged as an influential parameter that shapes nucleation kinetics, crystal growth, and particle uniformity (Camargo et al., 2015; Guo et al., 2023; Yang et al., 2024). Experimental comparisons have shown that reaction mixtures subjected to minimal stirring often produce smaller, more homogenous nanoparticles, while vigorous agitation increases particle size variability and promotes agglomeration (Ahmadi et al., 2024; Mirzanejad et al., 2025). Indeed, achieving an optimal particle size through controlled-stirring is important, as nanoparticles within the EPR-favorable size range are more efficiently retained within tumor tissue and therefore better positioned to support passive targeting in drug delivery (Deivayanai et al., 2025; Dolai et al., 2021; Kim et al., 2023). Reaction duration further governs the extent of drug incorporation, as longer synthesis times allow for progressive entrapment of drug molecules within the developing framework until saturation is reached (Ahmadi et al., 2024). However, excessive reaction periods can also risk drug diffusion out of the matrix or structural compromise of the carrier itself (Fahim et al., 2024; Gao et al., 2013). Characterization techniques such as powder x-ray diffraction (PXRD) and functional group analysis (FTIR) have proven critical in verifying structural integrity and confirming drug inclusion by identifying characteristic diffraction patterns and vibrational shifts associated with drug coordination (Chakraborty et al., 2024; Ge et al., 2022; Kaur et al., 2017; Nguyen et al., 2024; Tran et al., 2025; Wang et al., 2020).

Accordingly, this study reports the synthesis of mesalamine-loaded ZIF-8 nanoparticles (MES@nZIF-8) under systematically varied controlled-stirring conditions, with the aim of elucidating how reaction time and mixing influence crystallinity, encapsulation efficiency, and particle morphology. By aligning the physicochemical attributes of MES@nZIF-8 with the requirements for effective passive targeting and high drug loading, the present work seeks to advance the rational design of nanoscale delivery systems tailored to enhance mesalamine's therapeutic potential in cancer therapy.

MATERIALS AND METHODS

Materials and supplies

Zinc nitrate hexahydrate ($Zn(NO_3)_2{\cdot}6H_2O$; 99% purity), 2-methylimidazole (99% purity), mesalamine (MES; 99% purity), dimethyl sulfoxide (DMSO; 99.5% purity) were purchased from Sigma Aldrich. Methanol (≥99.9% purity) was acquired from R&M Chemicals. All chemicals were used as received without any further purification.

Synthesis of nano sized ZIF-8 (nZIF-8)

The synthesis of nZIF-8 was carried out *via* one-pot solvothermal reaction followed by previously reported method with a slight modification (Kamal et al., 2021). Specifically, 0.66 g of $Zn(NO_3)_2{\cdot}6H_2O$ and 0.3 g of 2-methylimidazole were weighed and each dissolved separately in 14.3 mL of methanol. The imidazole solution was gradually added to the zinc nitrate solution under continuous stirring at 500 rpm for 15 min, resulting in the formation of a milky white suspension. The suspension was then subjected to centrifugation at 10,000 rpm for 10 min, followed by washing with methanol for three times. Finally, the supernatant was discarded, and the precipitate was collected and dried in an oven at 40 °C for 24 h.

Encapsulation of MES within nZIF-8 (MES@nZIF-8)

0.66 g of $Zn(NO_3)_2{\cdot}6H_2O$ and 0.3 g of 2-methylimidazole were weighed and each dissolved separately in 14.3 mL of methanol (Kamal et al., 2021). Subsequently, the mesalamine solution (MES; 8 mg mL^{-1} in DMSO) was added into the zinc nitrate solution under continuous stirring at 500 rpm. After 15 min, the 2-methylimidazole solution was introduced into the resulting mixture, and the reaction time varied at 15 min, 24 h, 48 h and 72 h. The suspension was then centrifuged at 10,000 rpm for 10 min. The resulting precipitate was washed three times with methanol to remove impurities. Finally, after discarding the supernatant, the collected solid was dried in a vacuum oven at room temperature overnight.

Structural identification of nanoparticles

Crystallinity and phase identification were assessed by powder X-ray diffraction (PXRD) using a PANalytical X'Pert³ Powder diffractometer equipped with an image plate detector operating in continuous scan mode with Cu Kα radiation (λ = 1.540598 Å). Approximately 50 mg of each sample was loaded onto the holder and leveled with a spatula, and diffraction data were processed with X'Pert HighScore software. Functional groups were analyzed by Nicolet 6700 FTIR-ATR spectroscopy over 4000–400 cm^{-1} after cleaning the diamond stage with 70% ethanol; 1 g of sample was pressed onto the stage, and spectra were evaluated in Origin Pro 8.5. Thermal stability was examined by thermogravimetric analysis (TGA) on a PerkinElmer STA6000, heating samples from 50 to 800 °C at 10 °C min^{-1} under continuous nitrogen flow. Morphology was characterized by JEOL JSM-IT200 SEM after gold sputter-coating, with images acquired at 17 kV, a 10.2 mm working distance, and up to 50,000 magnifications. Particle size and shape were determined using ImageJ (v1.48). Hydrodynamic sizes were measured by dynamic light scattering (DLS; Zetasizer Nano ZS, Malvern) using an argon laser (λ = 488 nm) at a 173° scattering angle. Samples were prepared at a 1:9 (w/v) ratio in methanol and gently loaded into disposable polystyrene cuvettes to avoid air bubbles. Measurements were taken at 25 °C after 120 s of temperature equilibration.

Encapsulation efficiency and MES loading percentage

After the reaction mixture finished stirring, the supernatant was collected for analysis of MES loading capacity and encapsulation efficiency. This analysis was performed using Thermo Scientific GENESYS UV-vis spectrophotometer where the absorption detector for MES was set at 330 nm. The MES loading amount (ML%) and encapsulation efficiency (EE%) within nZIF-8 was calculated as follows: ML% = [amount of MES (mg) in nZIF-8/weight (mg) of nZIF-8] × 100 and EE% = [amount of MES (mg) in nZIF-8/amount of MES (mg) added during synthesis process] × 100.

RESULTS

Synthesis and structural identification

The synthesis of mesalamine-loaded nano-ZIF-8 (MES@nZIF-8) under controlled stirring was accomplished with varied reaction times of 15 min, 24 h, 48 h and 72 h. Visual observation (Figure 1) revealed a progressive color transition of the suspensions from milky white at the shortest reaction time to pale yellow at 72 h, suggestive of time-dependent changes occurring during the encapsulation process.

Powder X-ray diffraction analysis (PXRD) was used to assess the crystallinity and structural identification of the nanoparticles. The PXRD patterns of MES@nZIF-8 were compared with the theoretical pattern simulated for ZIF-8 as

shown in Figure 2A. The results revealed a series of distinct peaks at 7.4°, 10.4°, 12.7°, 14.7°, 16.4°, 18.0°, 22.1°, 24.5°, 26.7°, and 29.6°, corresponding to the (011), (002), (112), (022), (013), (222), (114), (233), (134), and (044) planes.

Fourier transformed infrared (FTIR) spectroscopy provided additional evidence confirming the effective encapsulation of MES within ZIF-8 nanoparticles. The pristine nZIF-8 FT-IR spectrum exhibited distinctive absorption bands serving as a baseline to assess the MES loaded nZIF-8. Specifically, absorption bands of ZIF-8 were found at: (i) 1576 cm^{-1} and within the 1430–1300 cm^{-1} range, attributed to the C=N bonds stretching and ring vibrations of 2-methylimidazole, respectively; (ii) 1145 and 994 cm^{-1} are associated with the stretching and bending of the C–N bonds within the ligand framework; (iii) 693 cm^{-1} represented the out-of-plane deformation of imidazole ring; and, whereas, (iv) 420 cm^{-1} was indicative of Zn–N bond stretching. These combined spectral features suggest the formation of coordination bonds between tetrahedral Zn^{2+} and 2-methylimidazolate-derived N atoms (Zhang, Jia, & Hou, 2018) (Figure 2B). After 48 h of MES loading, two new, strong peaks emerged at 2359 cm^{-1} and 2341 cm^{-1}, along with a peak at 1674 cm^{-1}, consistent with interactions between MES functional groups and the ZIF-8 framework, confirming successful encapsulation.

Similarly, TGA under N_2 flow, depicts a trend of MES@nZIF-8 with varied reaction time at 48 h < 72 h < 24 h < 15 min < nZIF-8 with respect to thermal stability (Figure 2C). MES@nZIF-8 begin to thermally decompose over the 130-490°C range whereas nZIF-8 is thermally stable up to at least 580 °C.

Figure 1

Visual appearance of MES@nZIF-8 synthesized under different reaction times

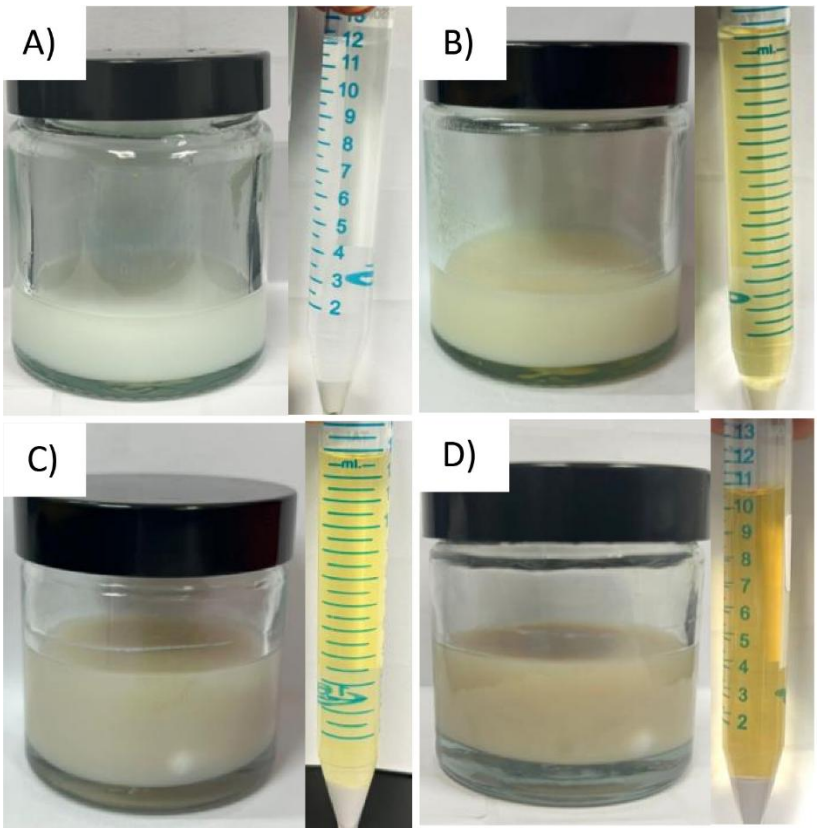

Note: MES@nZIF-8 suspensions synthesized at reaction times of 15 min (A), 24 h (B), 48 h (C), and 72 h (D), showing a gradual color change from milky white to yellow.

Scanning electron microscopy (SEM) provided further insight into the morphology of the nanoparticles (Figure 3). The pristine nZIF-8 displayed uniform octahedral crystals with smooth surfaces and narrow size distribution (91.2 ± 10.77nm). Upon encapsulation of MES, the particle size increased to 148.03 ± 19.12 nm (15 min), 186.37 ± 24.59 nm (24 h), 169.37 ± 25.86 nm (48 h), and 224.31 ± 31.10 nm (72 h). Consequently, partial agglomeration was apparent on 48 and 72 h reaction time.

The hydrodynamic sizes were obtained by dynamic light scattering (DLS), which is frequently employed due to its non-destructive technique to determine particle size in suspensions. The results revealed monomodal, narrow-size distributions for all samples (PDI ≈ 0.2; Figure 4). Pristine nZIF-8 showed an average hydrodynamic size of 229.97 ± 0.74 nm. Following MES encapsulation, size increased 20% with 272.57 ± 8.6 nm (15 min), 274.07 ± 4.49 nm (24 h), 266.70 ± 4.32 nm (48 h) and 288.40 ± 1.99 nm (72 h).

Figure 2

Structural characterization of nZIF-8 and MES@nZIF-8 synthesized under various reaction times

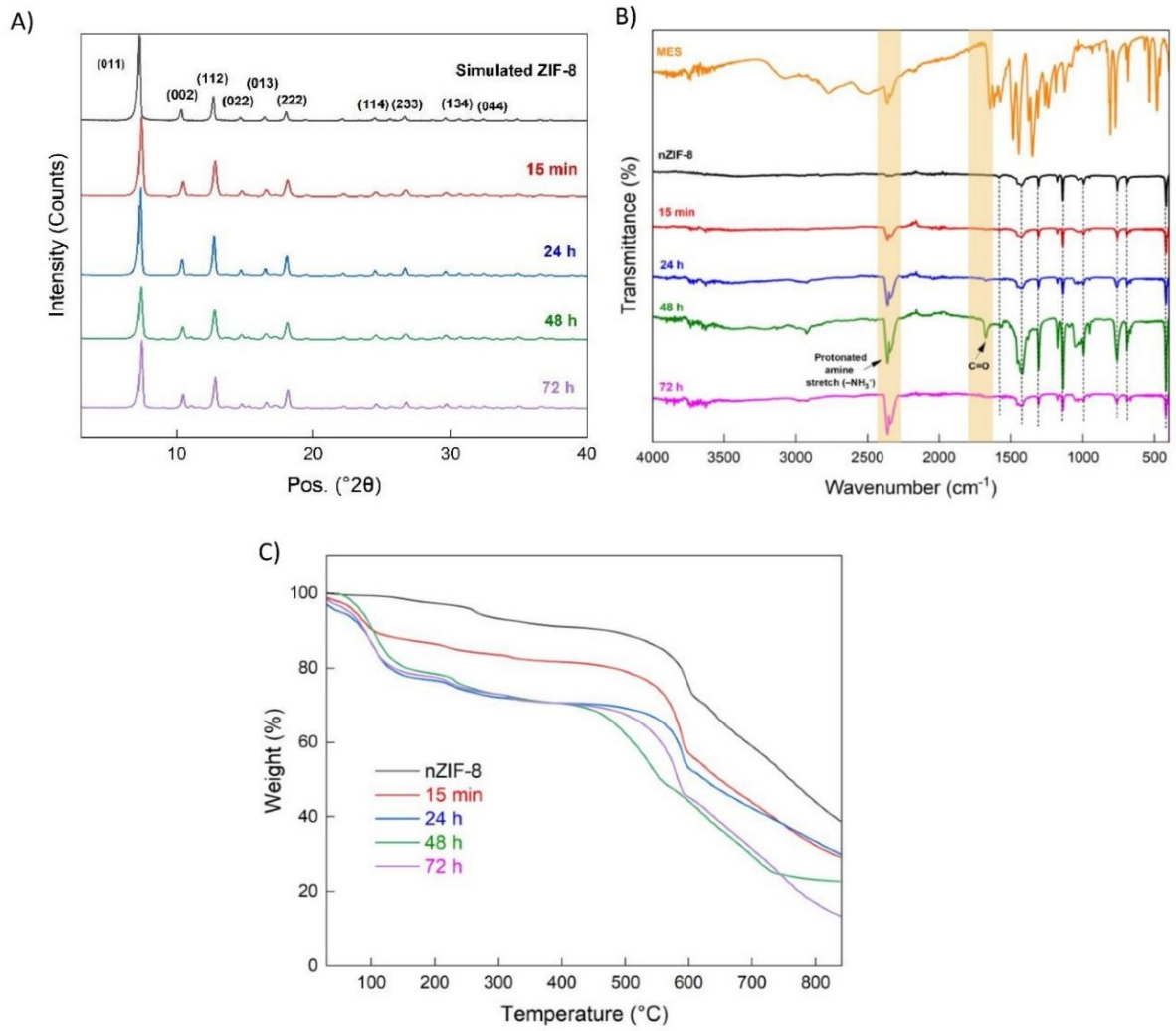

Note: Powder X-ray diffraction (PXRD) pattern (A), Fourier transform-infrared spectroscopy (FTIR) spectra (B) with orange highlights that directly related to the successful encapsulation of MES within nZIF-8, and Thermogravimetric analysis (TGA) profiles (C) of synthesized MES@nZIF-8 at 15 min (red), 24 h (blue), 48 h (green), and 72 h (purple) compared with the pristine nZIF-8 (black).

Encapsulation efficiency and MES loading percentage

Encapsulation efficiency and MES loading amount were quantified by UV–Vis spectrophotometric analysis of the supernatants (mean ± SD, *n* = 3). As summarized in Table 1, encapsulation efficiency exceeded 93% at all time points, peaking at 95.35 ± 0.02% after 48 h of stirring. Similarly, the MES loading increased from 10.00% (15 min) to 10.17% (48 h), before decreasing slightly to 10.03% (72 h).

Table 1

Encapsulation efficiency and MES loading (%) of MES@nZIF-8 over various reaction times

MES@nZIF-8	15 min	24 h	48 h	72 h
Encapsulation Efficiency (EE %)	93.74 ± 0.03	94.46 ± 0.01	95.35 ± 0.02	94.00 ± 0.01
MES Loading (ML %)	10.00	10.08	10.17	10.03

Note: Each value represents the mean ± standard deviation (SD) (n=3).

Figure 3

Scanning electron microscopy (SEM) images of synthesized nanoparticles

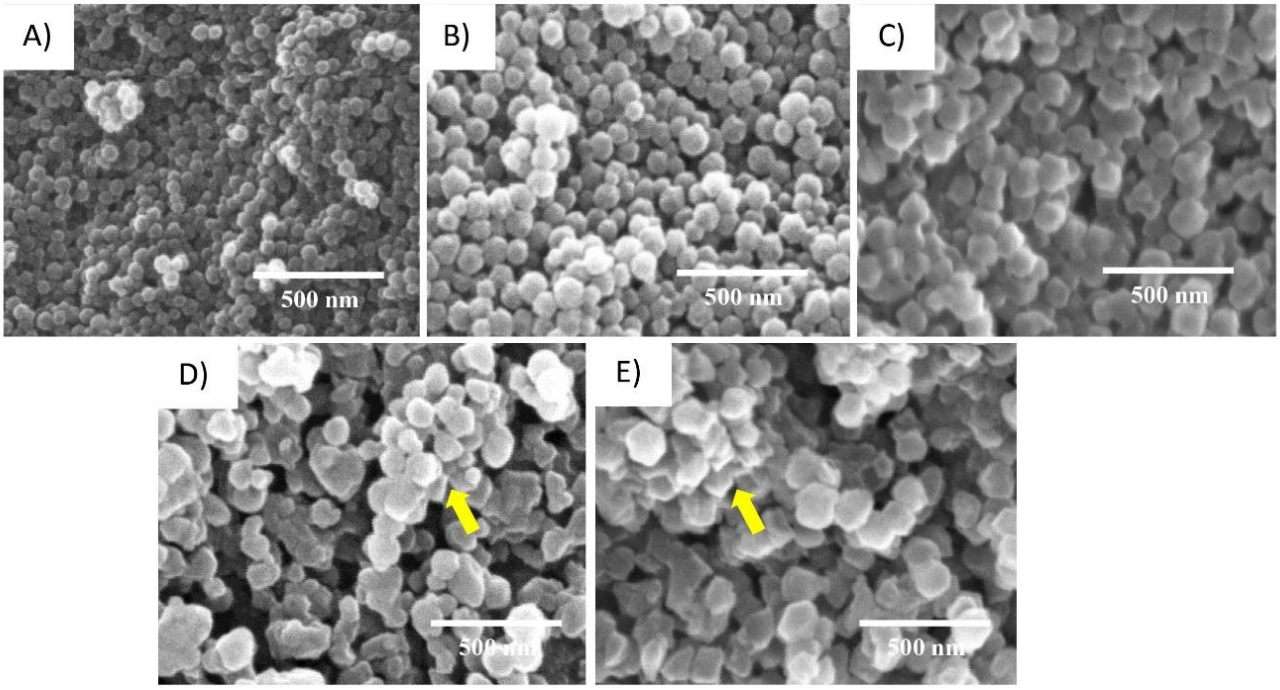

Note: Pristine nZIF-8 (A) and MES@nZIF-8 synthesized at different reaction times; 15 min (B), 24 h (C), 48 h (D) and 72 h (E). All nanoparticles exhibited ZIF-8 morphology, with variations in particle size and surface texture influenced by reaction time. Yellow arrows indicated particle agglomeration. Scale bar =500 nm.

Figure 4

Hydrodynamic size characterization of nZIF-8 and MES@nZIF-8 synthesized under various reaction times

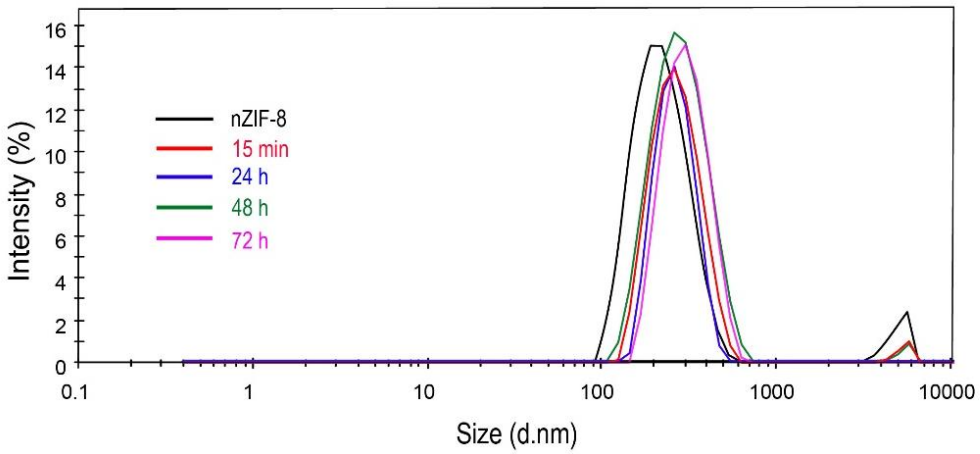

Note: Dynamic light scattering (DLS) size distributions for pristine nZIF-8 (black) and MES@nZIF-8 prepared for 15 min (red), 24 h (blue), 48 h (green), and 72 h (purple), showing a narrow primary population with hydrodynamic diameters <300 nm and a polydispersity index (PDI ≈ 0.2), indicative of good colloidal stability.

DISCUSSION

This study synthesized MES@nZIF-8 under controlled stirring conditions at various reaction times, providing a clear understanding of how synthesis duration impacts the structural integrity, morphology, and encapsulation characteristics of nanoparticles. As aforementioned, the observed color changes from milky white to pale yellow over time (Figure 1) suggested ongoing physicochemical interactions during MES encapsulation. These progressive hues shift are likely governed by the MES characteristics as they are highly susceptible to oxidative degradation due to the

presence of a 4-aminophenol structure (El Zein et al., 2023). We assumed that this color change reflects slow MES oxidation and interaction with the ZIF-8 framework during encapsulation, showing that the chemical environment of the nanoparticles was changing over time.

Once each nanoparticle was isolated, washed and dried, PXRD analysis was performed. As shown in Figure 2A, the diffraction patterns for synthesized MES@nZIF-8 were observed to be consistent with those of simulated ZIF-8. This PXRD analysis provides insight as MES encapsulation did not disrupt the crystallinity of the nZIF-8 structure. This robustness mirrors findings in other drug@ZIF-8 systems, incorporating hydrophobic and hydrophilic drugs, where XRD pattern showed no new peaks and maintained framework topology (Mazloum-Ardakani et al., 2023; Pandey et al., 2024).

Prior to further structural identification, the functional group analysis was defined by FTIR (Figure 2B). All nanoparticles exhibited the characteristic bands of pristine nZIF-8, suggesting that the original structure of nZIF-8 is well retained (Yong et al., 2024). It is important to first note that the observed bands of nZIF-8 are in accordance with those reported previously (Kamal et al., 2021; Silvaraju et al., 2025; Yong et al., 2024; Zhang, Jia, Li, et al., 2018). Interestingly, at 48 h, the strong intensity was observed at 2359 and 2341 cm^{-1} bands and additional peaks at 1674 cm^{-1}, corresponded to protonated amine ($–NH_3^+$) stretch of MES (Alam et al., 2019) and C=O bonds of its salicylic acid moiety (Deshmukh & Harwansh, 2021), respectively. These absent bands revealed clear evidence of the strong host-guest interactions between MES and nZIF-8.

Similarly, TGA provides several critical findings in MES encapsulation. As depicted in Figure 2C, the nanoparticles were extensively decomposed when encapsulated. The initial decomposition temperature of pure MES is 269°C (Urtiga et al., 2020). This remarkable decomposition occurred due to the MES decomposition inside the nZIF-8 framework, aligns with TGA study from previous research on ibuprofen loaded ZIF-8/Fe3O4 nanoparticles (Chakraborty et al., 2024).

Particle size and surface morphology of nanoparticles were observed via SEM (Figure 3). The particle size of MES@nzif-8 approximately doubled over time compared to pristine nZIF-8. The reasons are twofold: (i) MES absorbs onto the external surfaces of nZIF-8 (Kaur et al., 2017); and (ii) change in surface charge of ZIF-8 causing partial aggregation (Arumugam et al., 2025). Indeed, sizes within the range (20-500 nm) are favorable of EPR effects, allowing the nanoparticles to accumulate in tumor tissue for cancer targeting (Deivayanai et al., 2025). Notably, both pristine nZIF-8 and MES@nZIF-8 (15 min) maintained the smooth and rhombic morphology as reported earlier (Yahia et al., 2021), while longer stirring led to morphological changes and signs of agglomeration (Yong et al., 2024). It is important to note that agglomeration is not beneficial in this system; instead, it reflects reduced colloidal stability and loss of particle uniformity, thereby emphasize the need to limit stirring duration (Sevimli-Yurttas et al., 2024).

To transition from SEM to the dispersed state, particle size was assessed *via* DLS (Figure 4). All suspensions were monomodal with narrow distributions (PDI ≈ 0.2), indicates limited clustering in methanol (Danaei et al., 2018). The DLS trend follows the SEM observation: early samples retain the smooth, rhombic morphology, while longer stirring yields larger sizes and subtle signs of association. As expected, the hydrodynamic sizes were larger than SEM values. The increase observed by DLS is best explained by changes at the particle-solvent interface in dispersion, specifically formation of a hydrated MES corona and greater solvent binding at the surface, which raise the hydrodynamic diameter without generating secondary populations (Mittal et al., 2022; Wilson & Prud'homme, 2021).

Following confirmation of MES@nZIF-8's structural integrity, we proceeded to evaluate the encapsulation efficiency and MES loading over varying reaction times. Subsequently, at 48 h, > 95% of encapsulation efficiency and 10.17% loading was observed, likely arise from a balance between pore-filling kinetics and framework integrity by which extended stirring beyond 48 h, i.e 72 h, appeared to induce slight desorption or structural rearrangement (Caamaño et al., 2023). Although all nanoparticles achieved high encapsulation efficiencies, the loading amounts were determined to be relatively low (< 10%). This is a consequence of the limited amount of MES added during the synthesis (8 mg mL^{-1}) (Kamal et al., 2021). Despite this, the values of both encapsulation efficiency and loading amount remain acceptable for optimal therapeutic activity in inhibiting cancer progression, compared with other literature (Ding et al., 2024; Kumari et al., 2023; Namazi et al., 2024).

CONCLUSION

We have developed a rapid, one-pot stirring strategy for MES encapsulation within nano-ZIF-8 (MES@nZIF-8) that delivers high therapeutic payload without compromising framework integrity. PXRD analysis confirmed that the characteristic crystallinity of ZIF-8 was maintained across all synthesis conditions, validating the structural stability of the framework under the applied stirring regimes. SEM observations further demonstrated that particle morphology remained well-defined at shorter stirring durations, with agglomeration becoming evident only at extended reaction times. Although 48 h produced the highest encapsulation efficiency (>95%), moderate stirring durations provide a balance between encapsulation performance and colloidal stability. These findings offer valuable insight into the design of NSAID-loaded MOFs for enhanced anticancer efficacy and drug delivery applications. While the physicochemical characteristics and structural stability offered a strong foundation for understanding material performance and formulation robustness, the lack of *in vitro* and *in vivo* evaluations remain limited. Future investigations must address these biological dimensions to validate the potential of MES@nZIF-8 in clinical applications. Beyond mesalamine, this

controlled-stirring strategy offers promise for encapsulating a wider range of therapeutic molecules into ZIF-8, expanding its relevance for future drug-delivery applications.

AUTHOR CONTRIBUTIONS

Nur Airin Syahira Johari contributed to formal analysis, visualization, methodology, investigation, data curation, writing-original draft, review and editing. Gaayatri Silvaraju contributed to review and editing. Mohd Akmal Azhar contributed to data curation, supervision & writing-review. Azren Aida Asmawi contributed to data curation, supervision and writing-review. Rosniza Razali conducted the supervision and writing-review. Nurul Akmarina Mohd Abdul Kamal contributed to conceptualization, supervision, visualization, funding acquisition, writing-review and editing. All authors have given approval to the final version of the manuscript.

ETHICS APPROVAL

Not applicable.

FUNDING

This work was financially supported by internal funding under grant number RDU2303105 and Tabung Persidangan Dalam Negara (TPDN), Universiti Malaysia Pahang Al-Sultan Abdullah (UMPSA).

CONFLICT OF INTEREST

The authors declare no conflict of interest in this work.

ACKNOWLEDGEMENT

We extend our gratitude to Malaysian Nuclear Agency and Universiti Malaysia Pahang Al-Sultan Abdullah (UMPSA) for providing the research facilities essential to this work.

REFERENCES

Ahmadi, M., Asadian, E., Mosayebnia, M., Dadashzadeh, S., Shahhosseini, S., & Ghorbani-Bidkorpeh, F. (2024). Optimization of the synthesis and radiolabeling of ZIF-8 Nanoparticles. *Iran Journal of Pharmaceutical Research*, *23*(1). https://doi.org/10.5812/ijpr-144928

Alam, M. M., Tasneem, F., Kabir, A. L., & Rouf, A. S. S. (2019). Study of drug-drug and drug-food interactions of Mesalazine through FTIR and DSC. *Dhaka University Journal of Pharmaceutical Sciences*, *18*(2): 257–269. https://doi.org/10.3329/dujps.v18i2.44466

Amur, S. A., Soomro, N. A., Khuhro, Q., Wei, Y., Liang, H., & Yuan, Q. (2023). Encapsulation of natural drug gentiopicroside into zinc based Zeolitic Imidazolate Frameworks (ZIF-8): In-vitro drug release and improved antibacterial activity. *Journal of Drug Delivery Science and Technology*, *84*: 104530. https://doi.org/10.1016/j.jddst.2023.104530

Arumugam, K., Zochedh, A., Chandran, K., Sukumaran, S., Palaniyandi, K., Sultan, A. B., & Kathiresan, T. (2025). Influence of pyrazinamide loaded zeolite imidazole framework (ZIF-8) nanoparticles and effective anticancer effect in breast cancer cells. *Journal of Nanoparticle Research*, *27*(4): 94. https://doi.org/10.1007/s11051-025-06289-z

Beiranvand, M. (2021). A review of the biological and pharmacological activities of mesalazine or 5-aminosalicylic acid (5-ASA): an anti-ulcer and anti-oxidant drug. *Inflammopharmacology 29*(50): 1279–1290. https://doi.org/10.1007/s10787-021-00856-1

Biswas, S. (2021). Polymeric micelles as drug-delivery systems in cancer: challenges and opportunities. *Nanomedicine*, *16*(18): 1541–1544. https://doi.org/10.2217/nnm-2021-0081

Caamaño, K., López-Carballo, G., Heras-Mozos, R., Glatz, J., Hernández-Muñoz, P., Gavara, R., & Giménez-Marqués, M. (2023). ZIF-8 encapsulation improves the antifungal activity of benzaldehyde and methyl anthranilate in films. *Dalton Transactions*, *52*(47): 17993–17999. https://doi.org/10.1039/d3dt03229a

Camargo, P. H. C., Rodrigues, T. S., da Silva, A. G. M., & Wang, J. (2015). Controlled synthesis: nucleation and growth in solution. In: Xiong, Y., Lu, X. (eds) *Metallic Nanostructures*. Springer, Cham. https://doi.org/10.1007/978-3-319-11304-3_2

Chakraborty, A., Nandi, R., Kumar, D., & Acharya, H. (2024). Investigation on the drug release efficacy of the ibuprofen-loaded ZIF-8/Fe3O4 NPs nanocarrier. *ACS Omega 9*(30): 32418-32428. https://doi.org/10.1021/acsomega.3c09135

Chehelgerdi, M., Chehelgerdi, M., Allela, O. Q. B., Pecho, R. D. C., Jayasankar, N., Rao, D. P., Thamaraikani, T., Vasanthan, M., Viktor, P., Lakshmaiya, N., Saadh, M. J., Amajd, A., Abo-Zaid, M. A., Castillo-Acobo, R. Y., Ismail, A. H., Amin, A. H., & Akhavan-Sigari, R. (2023). Progressing nanotechnology to improve targeted cancer treatment: overcoming hurdles in its clinical implementation. *Molecular Cancer 22*(1). https://doi.org/10.1186/s12943-023-01865-0

Chelliah, R., Rubab, M., Vijayalakshmi, S., Karuvelan, M., Barathikannan, K., & Oh, D. H. (2025). Liposomes for drug delivery: classification, therapeutic applications, and limitations. *Next Nanotechnology*, *8*: 100209. https://doi.org/10.1016/j.nxnano.2025.100209

Cheng, B., & Xu, P. (2020). Chapter 13 - Nanoparticle-based formulation for drug repurposing in cancer treatment. *Drug Repurposing in Cancer Therapy: Approaches and Applications* (pp. 335–351). Elsevier. https://doi.org/10.1016/b978-0-12-819668-7.00013-0

Danaei, M., Dehghankhold, M., Ataei, S., Hasanzadeh Davarani, F., Javanmard, R., Dokhani, A., Khorasani, S., & Mozafari, M. R. (2018). Impact of particle size and polydispersity index on the clinical applications of lipidic nanocarrier systems. *Pharmaceutics*, *10*(2): 57. https://doi.org/10.3390/pharmaceutics10020057

Deivayanai, V. C., Thamarai, P., Karishma, S., Saravanan, A., Yaashikaa, P. R., Vickram, A. S., Hemavathy, R. V., Kumar, R. R., Rishikesavan, S., & Shruthi, S. (2025). Advances in nanoparticle-mediated cancer therapeutics: current research and future perspectives. *Cancer Pathogenesis and Therapy*, *3*(4): 293–308. https://doi.org/10.1016/J.CPT.2024.11.002

Deshmukh, R., & Harwansh, R. K. (2021). Preformulation considerations development and evaluation of mesalamine loaded polysaccharide-based complex mucoadhesive beads for colon targeting. *Indian Journal of Pharmaceutical Education and Research*, *55*(1): 95–106. https://doi.org/10.5530/ijper.55.1.13

Ding, L., Chen, H., Bi, G., Wang, W., & Li, R. (2024). Improved anti-cancer effects of luteolin@ZIF-8 in cervical and prostate cancer cell lines. *Heliyon*, *10*(6): e28232. https://doi.org/10.1016/j.heliyon.2024.e28232

Dolai, J., Mandal, K., & Jana, N. R. (2021). Nanoparticle size effects in biomedical applications. *ACS Applied Nano Materials*, *4*(7): 6471–6496. https://doi.org/10.1021/acsanm.1c00987

El Zein, R., Ispas-Szabo, P., Jafari, M., Siaj, M., & Mateescu, M. A. (2023). Oxidation of mesalamine under phenoloxidase- or peroxidase-like enzyme catalysis. *Molecules*, *28*(24). https://doi.org/10.3390/molecules28248105

Estrella, V., Chen, T., Lloyd, M., Wojtkowiak, J., Cornnell, H. H., Ibrahim-Hashim, A., Bailey, K., Balagurunathan, Y., Rothberg, J. M., Sloane, B. F., Johnson, J., Gatenby, R. A., & Gillies, R. J. (2013). Acidity generated by the tumor microenvironment drives local invasion. *Cancer Research*, *73*(5): 1524–1535. https://doi.org/10.1158/0008-5472.can-12-2796

Fahim, M., Shahzaib, A., Nishat, N., Jahan, A., Bhat, T. A., & Inam, A. (2024). Green synthesis of silver nanoparticles: a comprehensive review of methods, influencing factors, and applications. *JCIS Open, 16: 100125.* https://doi.org/10.1016/j.jciso.2024.100125

Gao, L., Liu, G., Ma, J., Wang, X., Zhou, L., Li, X., & Wang, F. (2013). Application of drug nanocrystal technologies on oral drug delivery of poorly soluble drugs. *Pharmaceutical Research 30*(2): 307–324. https://doi.org/10.1007/s11095-012-0889-z

Ge, Y., Wang, K., Liu, J., Tian, Y., Li, H., Wang, H. Z., Lin, Z., Qiu, M., & Tang, B. (2022). A ZIF-8-based multifunctional intelligent drug release system for chronic osteomyelitis. *Colloids and Surfaces B: Biointerfaces*, *212*. https://doi.org/10.1016/j.colsurfb.2022.112354

Guo, M., Cui, W., Li, Y., Fei, S., Sun, C., Tan, M., & Su, W. (2023). Microfluidic fabrication of size-controlled nanocarriers with improved stability and biocompatibility for astaxanthin delivery. *Food Research International*, *170*: 112958. https://doi.org/10.1016/J.FOODRES.2023.112958

Haripriyaa, M., & Suthindhiran, K. (2023). Pharmacokinetics of nanoparticles: current knowledge, future directions and its implications in drug delivery. *Future Journal of Pharmaceutical Sciences*, *9*(1). https://doi.org/10.1186/s43094-023-00569-y

Kalyane, D., Raval, N., Maheshwari, R., Tambe, V., Kalia, K., & Tekade, R. K. (2019). Employment of enhanced permeability and retention effect (EPR): Nanoparticle-based precision tools for targeting of therapeutic and diagnostic agent in cancer. *Materials Science and Engineering: C*, *98*: 1252–1276. https://doi.org/10.1016/j.msec.2019.01.066

Kamal, N. A. M. A., Abdulmalek, E., Fakurazi, S., Cordova, K. E., & Abdul Rahman, M. B. (2021). Surface peptide functionalization of zeolitic imidazolate framework-8 for autonomous homing and enhanced delivery of chemotherapeutic agent to lung tumor cells. *Dalton Transactions*, *50*(7): 2375–2386. https://doi.org/10.1039/d1dt00116g

Kaur, H., Mohanta, G. C., Gupta, V., Kukkar, D., & Tyagi, S. (2017). Synthesis and characterization of ZIF-8 nanoparticles for controlled release of 6-mercaptopurine drug. *Journal of Drug Delivery Science and Technology*, *41*: 106–112. https://doi.org/10.1016/j.jddst.2017.07.004

Khalil, N. A., Ahmed, E. M., Tharwat, T., & Mahmoud, Z. (2024). NSAIDs between past and present; a long journey towards an ideal COX-2 inhibitor lead. *RSC Advances 14*(42): 30647–30661. https://doi.org/10.1039/d4ra04686b

Kim, J., Cho, H., Lim, D.-K., Joo, M. K., & Kim, K. (2023). Perspectives for improving the tumor targeting of nanomedicine via the EPR effect in clinical tumors. *International Journal of Molecular Sciences*, *24*(12): 10082. https://doi.org/10.3390/ijms241210082

Kolawole, O. R., & Kashfi, K. (2022). NSAIDs and cancer resolution: new paradigms beyond cyclooxygenase. *International Journal of Molecular Sciences 23*(3). https://doi.org/10.3390/ijms23031432

Kumari, P. P. N. C., Asadevi, H., Vindhya, P. S., Kavitha, V. T., Nair, A. S., & Raghunandan, R. (2023). Development of a Cu/ZnO@ZIF-8 nanocomposite as a pH-responsive drug delivery vehicle for the sustained release of doxorubicin in human lung cancer cell lines. *Journal of Drug Delivery Science and Technology*, *90*: 105147. https://doi.org/10.1016/j.jddst.2023.105147

Lai, H., Liu, Y., Wu, J., Cai, J., Jie, H., Xu, Y., & Deng, S. (2022). Targeting cancer-related inflammation with non-steroidal anti-inflammatory drugs: Perspectives in pharmacogenomics. *Frontiers in Pharmacology 13*: 1078766. https://doi.org/10.3389/fphar.2022.1078766

Liefferinckx, C., Verstockt, B., Gils, A., Noman, M., Van Kemseke, C., Macken, E., De Vos, M., Van Moerkercke, W., Rahier, J.-F., Bossuyt, P., Dutré, J., Humblet, E., Staessen, D., Peeters, H., Van Hootegem, P., Louis, E., Franchimont, D., Baert, F., Vermeire, S., & Belgian Inflammatory Bowel Disease Research and Development Group [BIRD group]. (2019). Long-term clinical effectiveness of ustekinumab in patients with crohn's disease who failed biologic therapies: a national cohort study. *Journal of Crohn's and Colitis*, *13*(11): 1401–1409. https://doi.org/10.1093/ecco-jcc/jjz080

Lim, S., Park, J., Shim, M. K., Um, W., Yoon, H. Y., Ryu, J. H., Lim, D. K., & Kim, K. (2019). Recent advances and challenges of repurposing nanoparticle-based drug delivery systems to enhance cancer immunotherapy. *Theranostics 9*(25):7906–7923. https://doi.org/10.7150/thno.38425

Mazloum-Ardakani, M., Shaker-Ardakani, N., & Ebadi, A. (2023). Development of metal–organic frameworks (ZIF-8) as low-cost carriers for sustained release of hydrophobic and hydrophilic drugs: in vitro evaluation of anti-breast cancer and anti-infection effect. *Journal of Cluster Science*, *34*(4): 1861–1876. https://doi.org/10.1007/s10876-022-02349-9

Mirzanejad, S., Bagherzadeh, M., Bayrami, A., Daneshgar, H., Bahrami, A., & Mahdavi, M. (2025). Improving the drug delivery performance of ZIF-8 with amine functionalization as a 5-fluorouracil nanocarrier. *Scientific Reports*, *15*(1). https://doi.org/10.1038/s41598-025-03542-2

Mittal, A., Gandhi, S., & Roy, I. (2022). Mechanistic interaction studies of synthesized ZIF-8 nanoparticles with bovine serum albumin using spectroscopic and molecular docking approaches. *Scientific Reports*, *12*(1). https://doi.org/10.1038/s41598-022-14630-y

Namazi, H., Moghadam, M. R., & Karimi, S. (2024). A biocompatible drug controlled release system based on β-cyclodextrin crosslinked magnetic lactose/ZIF-8 metal-organic frameworks for cancer treatment. *Colloids and Surfaces A: Physicochemical and Engineering Aspects*, *703*: 135227. https://doi.org/10.1016/j.colsurfa.2024.135227

Nguyen, H. V. T., Pham, S. N., Mirzaei, A., Mai, N. X. D., Nguyen, C. C., Thi Nguyen, H., Vong, L. B., Nguyen, P. T., & Doan, T. L. H. (2024). Surface modification of ZIF-8 nanoparticles by hyaluronic acid for enhanced targeted delivery of quercetin. *Colloids and Surfaces A: Physicochemical and Engineering Aspects*, *696*: 134288. https://doi.org/10.1016/j.colsurfa.2024.134288

Obaid, E. A. M. S., Wu, S., Zhong, Y., Yan, M., Zhu, L., Li, B., Wang, Y., Wu, W., & Wang, G. (2022). pH-responsive hyaluronic acid-enveloped ZIF-8 nanoparticles for anti-atherosclerosis therapy. *Biomaterials Science*, *10*(17): 4837–4847. https://doi.org/10.1039/d2bm00603k

Ortega, E., Ruiz, M. A., Peralta, S., Russo, G., & Morales, M. E. (2020). Improvement of mesoporous silica nanoparticles: A new approach in the administration of NSAIDS. *Journal of Drug Delivery Science and Technology*, *58*. https://doi.org/10.1016/j.jddst.2020.101833

Ozleyen, A., Yilmaz, Y. B., Donmez, S., Atalay, H. N., Antika, G., & Tumer, T. B. (2023). Looking at NSAIDs from a historical perspective and their current status in drug repurposing for cancer treatment and prevention. *Journal of Cancer Research and Clinical Oncology*, *149*(5): 2095–2113. https://doi.org/10.1007/s00432-022-04187-8

Pandey, S. K., Sharmah, B., Manna, P., Chawngthu, Z., Kumar, S., Trivedi, A. K., Saha, S. K., & Das, J. (2024). Fabrication of hydrophobic drug-loaded Zeolitic Imidazolate Framework-8 (ZIF-8) for enhanced anti-bacterial activity. *Journal of Molecular Structure*, *1312*: 138452. https://doi.org/10.1016/j.molstruc.2024.138452

Qian, J., Guo, Y., Xu, Y., Wang, X., Chen, J., & Wu, X. (2023). Combination of micelles and liposomes as a promising drug delivery system: a review. *Drug Delivery and Translational Research*, *13*(11): 2767–2789. https://doi.org/10.1007/s13346-023-01368-x

Sevimli-Yurttas, Z., Moreira, R. G., & Castell-Perez, E. (2024). Aggregation and sedimentation stability of nanoscale zeolitic imidazolate framework (ZIF-8) nanocomposites for antimicrobial agent delivery applications. *Nano Select*, *5*(12). https://doi.org/10.1002/nano.202400029

Silvaraju, G., Johari, N. A. S., Asmawi, A. A., Razali, R., Adam, F., Shan, Y. L., & Kamal, N. A. M. A. (2025). Hyaluronic acid-functionalized zeolitic imidazolate framework-8 nanoparticles: a one-pot synthesis approach for breast cancer therapy. *Journal of Nanoparticle Research*, *27*(8): 215. https://doi.org/10.1007/s11051-025-06412-0

Słoka, J., Madej, M., & Strzalka-Mrozik, B. (2023). Molecular mechanisms of the antitumor effects of mesalazine and its preventive potential in colorectal cancer. *Molecules, 28*(13). https://doi.org/10.3390/molecules28135081

Tafech, A., & Stéphanou, A. (2024). On the importance of acidity in cancer cells and therapy. *Biology*, *13*(4): 225. https://doi.org/10.3390/biology13040225

Tran, T. Van, Dang, H. H., Nguyen, H., Nguyen, N. T. T., Nguyen, D. H., & Nguyen, T. T. T. (2025). Synthesis methods, structure, and recent trends of ZIF-8-based materials in the biomedical field. *Nanoscale Advances 7*(13): 3941-3960. https://doi.org/10.1039/d4na01015a

Tunc, C. U., Kursunluoglu, G., Akdeniz, M., Kutlu, A. U., Han, M. I., Yerer, M. B., & Aydin, O. (2023). Investigation of gold nanoparticle naproxen-derived conjugations in ovarian cancer. *ACS Materials Au*, *3*(5): 483–491. https://doi.org/10.1021/acsmaterialsau.3c00033

Urtiga, S. C. da C., Alves, V. M. O., Melo, C. de O., Lima, M. N. de, Souza, E., Cunha, A. P., Ricardo, N. M. P. S., Oliveira, E. E., & Egito, E. S. T. do. (2020). Xylan microparticles for controlled release of mesalamine: Production and physicochemical characterization. *Carbohydrate Polymers*, *250*: 116929. https://doi.org/10.1016/j.carbpol.2020.116929

Vagena, I. A., Malapani, C., Gatou, M. A., Lagopati, N., & Pavlatou, E. A. (2025). Enhancement of EPR effect for passive tumor targeting: current status and future perspectives. *Applied Sciences (Switzerland)*, *15*(6). https://doi.org/10.3390/app15063189

Wang, Q., Sun, Y., Li, S., Zhang, P., & Yao, Q. (2020). Synthesis and modification of ZIF-8 and its application in drug delivery and tumor therapy. *RSC Advances 10*(62): 37600–37620. https://doi.org/10.1039/d0ra07950b

Webb, B. A., Chimenti, M., Jacobson, M. P., & Barber, D. L. (2011). Dysregulated pH: a perfect storm for cancer progression. *Nature Reviews Cancer*, *11*(9): 671–677. https://doi.org/10.1038/nrc3110

Wilson, B. K., & Prud'homme, R. K. (2021). Nanoparticle size distribution quantification from transmission electron microscopy (TEM) of ruthenium tetroxide stained polymeric nanoparticles. *Journal of Colloid and Interface Science*, *604*: 208–220. https://doi.org/10.1016/J.JCIS.2021.04.081

Xie, H., Liu, X., Huang, Z., Xu, L., Bai, R., He, F., Wang, M., Han, L., Bao, Z., Wu, Y., Xie, C., & Gong, Y. (2022). Nanoscale zeolitic imidazolate framework (ZIF)–8 in cancer theranostics: current challenges and prospects. *Cancers 14*(16). https://doi.org/10.3390/cancers14163935

Yahia, M., Phan Le, Q. N., Ismail, N., Essalhi, M., Sundman, O., Rahimpour, A., Dal-Cin, M. M., & Tavajohi, N. (2021). Effect of incorporating different ZIF-8 crystal sizes in the polymer of intrinsic microporosity, PIM-1, for CO_2/CH_4 separation. *Microporous and Mesoporous Materials*, *312*: 110761. https://doi.org/10.1016/j.micromeso.2020.110761

Yang, Y., Hao, J., & Cui, J. (2024). Engineering of hierarchical mesoporous silica nanoparticles via control over surfactant nanoarchitectonics for biological applications. *Current Opinion in Colloid & Interface Science*, *72*: 101819. https://doi.org/10.1016/j.cocis.2024.101819

Yao, Y., Zhou, Y., Liu, L., Xu, Y., Chen, Q., Wang, Y., Wu, S., Deng, Y., Zhang, J., & Shao, A. (2020). Nanoparticle-based drug delivery in cancer therapy and its role in overcoming drug resistance. *Frontiers in Molecular Biosciences 7*. https://doi.org/10.3389/fmolb.2020.00193

Yong, L. X., Malek, M. I. A., Asmawi, A. A., Razali, R., Azil, A., Yusoh, N. A., & Kamal, N. A. M. A. (2024). Biological evaluation of folic acid functionalized nano-zeolitic imidazolate framework-8 for cancer therapy. *Colloid and Polymer Science 303*: 443–456. https://doi.org/10.1007/s00396-024-05357-5

Zafar, A., Khatoon, S., Khan, M. J., Abu, J., & Naeem, A. (2025). Advancements and limitations in traditional anti-cancer therapies: a comprehensive review of surgery, chemotherapy, radiation therapy, and hormonal therapy. *Discover Oncology 16*(1). https://doi.org/10.1007/s12672-025-02198-8

Zhang, Y., Jia, Y., & Hou, L. (2018). Synthesis of zeolitic imidazolate framework-8 on polyester fiber for $PM_{2.5}$ removal. *RSC Advances, 8*(55): 31471–31477. https://doi.org/10.1039/c8ra06414h

Zhang, Y., Jia, Y., Li, M., & Hou, L. (2018). Influence of the 2-methylimidazole/zinc nitrate hexahydrate molar ratio on the synthesis of zeolitic imidazolate framework-8 crystals at room temperature. *Scientific Reports, 8*(1). https://doi.org/10.1038/s41598-018-28015-7

Citation:

Johari, N. A. S., Silvaraju, G., Azhar, M. A., Asmawi, A. A., Razali, R., & Mohd Abdul Kamal, N. A. (2026). Development and characterization of mesalamine-loaded nano-ZIF-8 via controlled-stirring synthesis. *Life Sciences, Medicine and Biomedicine*, *10*(1). https://doi.org/10.28916/lsmb.10.1.2026.227

Life Sciences, Medicine and Biomedicine
ISSN: 2600-7207